

# A Micro-Grid Energy Management Strategy Integrating Photovoltaic Energy Prediction<sup>\*</sup>

Daniele Ioli<sup>\*</sup> Alessandro Falsone<sup>\*</sup> Axel Busboom<sup>\*\*</sup>  
Maria Prandini<sup>\*</sup>

<sup>\*</sup>*Politecnico di Milano, Italy (e-mail: name.surname@polimi.it)*

<sup>\*\*</sup>*Munich University of Applied Sciences, Germany  
(e-mail: axel.busboom@hm.edu)*

---

**Abstract:** This paper deals with the integration in the electrical grid of distributed generation from renewables through energy management operations at the micro-grid level. We consider a micro-grid with a solar power plant and propose an energy management strategy that sets the energy exchange with the main grid during a one-day time horizon so as to minimize the electrical energy costs. In order to counteract uncertainty, the proposed strategy implements a predictive approach that decides at each time step how to operate the micro-grid on the residual time horizon based on a forecast of the photovoltaic energy production. To this purpose, we introduce a predictor of the photovoltaic energy production that is designed based on historical data. Validation on a testbed and simulation results show that the proposed method is promising.

*Keywords:* Smart grid, energy management, solar energy prediction, predictive control.

---

## 1. INTRODUCTION

A micro-grid comprises interconnected loads, generators, and storage systems, and can operate in either islanded or grid-connected mode. In the latter configuration, the main grid supplies power to the micro-grid in case of a deficit and absorbs power in case of generated power excess. Time-varying electrical energy prices are imposed by the main grid as an incentive for the micro-grid to adopt an energy management strategy and shift the power request from peak hours of demand (when the price is set high by the main grid) to hours of low demand (when the price is set low). As a result, a micro-grid that implements an optimal energy management strategy is contributing to the main grid stabilization.

In a micro-grid setting where loads are non deferrable and power generation is obtained from renewable energy sources, Electric Storage Systems (ESSs) are fundamental to energy management operations, Zamora and Srivastava (2010). By shifting in time the load demand, ESSs can realize a deferrable virtual load and allow to buy energy not on load request, but when the price is lower, thus reducing costs. They can smooth the mismatch in production/consumption by storing energy when the production exceeds the demand and providing energy when the production is insufficient to meet the loads demand. They can act as energy buffer and absorb fluctuations in the renewable energy production (see, e.g., Teleke et al. (2010), Xie et al. (2012) were they are integrated in a wind farm). They can be used for optimizing the dispatch of energy produced from renewables, Garcia and Bordons (2013), or

to track some energy exchange profile agreed with the grid, Ioli et al. (2017).

A major challenge in micro-grid optimization is dealing with uncertainty due to generation from renewable sources, Olivares et al. (2014). For instance, photovoltaic energy production can be highly variable from day to day, which prompts the need of devising suitable prediction strategies to be integrated within the energy management policy, Wan et al. (2015). Despite the large amount of effort in the literature on micro-grid energy management, Zia et al. (2018), there are only a few approaches in the literature that take into account uncertainty. As pointed out in Olivares et al. (2014), uncertainty is naturally accounted for in Model Predictive Control (MPC). In MPC, at each time-step an appropriately defined optimization problem is solved to compute the control actions over a pre-defined time horizon, then only the first control action is implemented, and the process is repeated at the subsequent time-steps. A prediction of the future behavior of the system initialized at the current state is used in the optimization problem formulation, which makes MPC a feedback control strategy able to counteract disturbances but only indirectly, because of their effect on the state value. This is the approach pursued in the recent paper Pippia et al. (2018), where micro-grid energy management is addressed via MPC assuming known disturbances and optimizing at each time step the parameters of a control policy.

In stochastic MPC (see Mesbah (2016) for a survey) disturbances are accounted for explicitly in the choice of the control action. However, they are typically assumed to be white noise processes so that past observations cannot

---

<sup>\*</sup>This work was partly supported by the European Commission under the UnCoVerCPS project, grant number 643921.

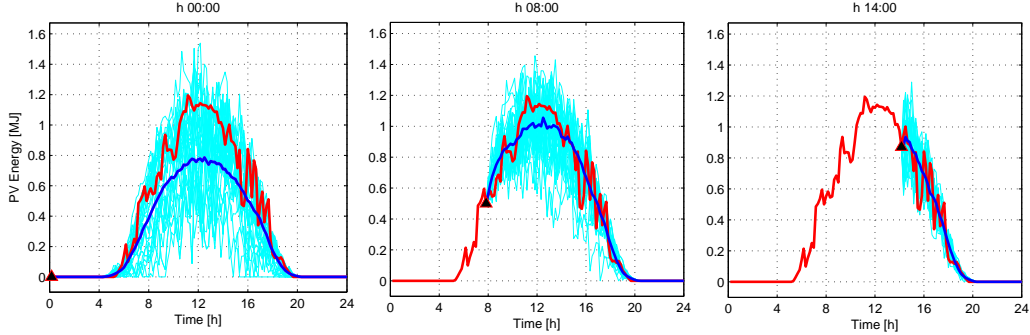


Fig. 1. Expected value of the future photovoltaic energy production (blue line) and profiles extracted at random from the a-posterior distribution (cyan lines) over 10-minute time slots: at midnight when no measurements are available (plot on the left); at 8 in the morning (plot in the middle) and at 14 in the afternoon (plot on the right) of the actual production profile (red line).

provide any information on their future realization, and hence no forecasting mechanism is put in place.

In this paper, we consider a simple grid-connected micro-grid with a non-deferrable load, a photovoltaic panel installation, and a storage system, and propose a predictive approach to energy management integrating a predictor of the photovoltaic energy production. Given the (stochastic) periodicity characterizing the photovoltaic energy production, we refer to a one-day time horizon, which is discretized into  $M$  time slots. During each time slot  $k$ , the energy exchange with the storage is chosen so as to minimize the electrical energy cost on the residual time horizon based on the most recent prediction of the photovoltaic energy production. The adopted photovoltaic energy time series predictor is built from historical data, and, hence, belongs to the class of so-called statistical approaches (see the review in Wan et al. (2015)). It is based on functional data analysis, Ramsay (2006), as the approach in Manganini et al. (2017) for the generation of stochastic power consumption profiles. The proposed strategy was implemented on a testbed at General Electric Global Research Center (GERC) in Munich, Germany, and compared against two strategies: a best (ideal) strategy, where the photovoltaic energy production is a-priori known, and a commonly adopted heuristic strategy, where the storage is charged if the energy production exceeds the demand and discharged if the demand exceeds the production, as if the overall system was operated in islanded mode. Data used in this paper appeared in Ioli et al. (2017).

## 2. ENERGY MANAGEMENT STRATEGY

We address energy management over a one-day horizon for a simple micro-grid connected to the main grid and composed of a non-deferrable load, a photovoltaic power plant, and a battery. This obviously simplified framework is representative of a broader class of micro-grid configurations, where, for instance, multiple loads are present and their requests are summed up in a larger equivalent load. Without loss of generality, we neglect the uncertainty in demand and describe the load as deterministic (see Remark 1). The price of electricity is typically time varying within the day, with a higher value for the price to buy with respect to the price to sell. Our goal is to appropriately set the energy flow with the battery so as to minimize the cost

for energy exchange with the main grid along the one-day time horizon, with the understanding that a negative cost means that the micro-grid is earning some money.

The reference one-day time horizon is discretized into  $M$  time frames of length  $\Delta t$ , i.e.,  $[k\Delta t, (k+1)\Delta t)$ ,  $k = 0, \dots, M-1$ . On each time frame  $k \in \{0, \dots, M-1\}$ , the energy  $g(k)$  exchanged with the main grid is given by the following balance equation

$$g(k) = \ell(k) - d(k) + u(k), \quad (1)$$

where  $\ell(k)$ ,  $d(k)$ ,  $u(k)$  represent, respectively, the electrical load energy request, the energy produced by the solar panels, and the energy exchanged with the storage in the time frame  $k$ . If  $g(k) > 0$ , then the main grid provides energy to the micro-grid, while if  $g(k) < 0$ , then the micro-grid sells energy to the main grid. The solar energy term  $d(k)$  can be viewed as a stochastic disturbance, whilst the energy exchanged with the battery  $u(k)$  is the control input, with  $u(k) > 0$  if the battery is charged in the time slot  $k$ ,  $u(k) < 0$  if discharged.

For the battery management, we propose to adopt a model predictive control-like approach where at each step  $t$ ,  $t = 0, \dots, M-1$ , the predicted value of the energy cost  $\hat{g}(k|t-1)$  for the residual time horizon  $k \in [t, M-1]$  is minimized. This entails building a predictor  $\hat{d}(k|t-1)$ ,  $k = t, \dots, M-1$ , of the future photovoltaic energy production given the past observations  $\{d(0), \dots, d(t-1)\}$ , and then computing

$$\hat{g}(k|t-1) = \ell(k) - \hat{d}(k|t-1) + u(k), \quad (2)$$

$k = t, \dots, M-1$ . The idea is that as we collect more and more observations on the solar energy production profile during the day, the predicted values get closer and closer to the actual profile (see Figure 1).

We model the storage system as a linear system with two inputs that cannot be active simultaneously and correspond to either charging or discharging the storage. More precisely, the stored energy  $U$  evolves according to

$$U(k+1) = aU(k) + \varepsilon_c u_c(k) - \varepsilon_d u_d(k), \quad (3)$$

where  $u_c(k)$  and  $u_d(k)$  are respectively the charging and discharging energy inputs in the time slot  $k$  of duration  $\Delta t$  and the re-scaling coefficients  $\varepsilon_c \in (0, 1)$  and  $\varepsilon_d \in (1, 2)$  account for the round trip efficiency of the battery. In the symmetric case  $\varepsilon_c = 1 - \varepsilon_u$  and  $\varepsilon_d = 1 + \varepsilon_u$  with  $\varepsilon_u \in (0, 1)$ .

Parameter  $a \in (0, 1)$  in (3) accounts for the self discharging of the storage (Faradaic efficiency).

Note that  $u(k) = u_c(k) - u_d(k)$  represents the energy fed into ( $u(k) > 0$ ) or drawn from ( $u(k) \leq 0$ ) the storage. Model (3) is valid when the state of charge (SOC) of the storage is within 5% and 95% of the maximum capacity  $\bar{U}$ , which translates into the constraint

$$0.05\bar{U} \leq U(k+1) \leq 0.95\bar{U}, \quad k = 0, \dots, M-1. \quad (4)$$

For  $k = 0, \dots, M-1$ , the energy exchanged with the storage is subject to the following constraints

$$0 \leq u_c(k) \leq u_{c,\max}, \quad 0 \leq u_d(k) \leq u_{d,\max} \quad (5)$$

$$u_c(k)u_d(k) \leq 0, \quad (6)$$

where  $u_{c,\max}$  ( $u_{d,\max}$ ) defines the maximum charge (discharge) energy exchange with the battery and the last constraint is imposed to avoid simultaneous charging and discharging. Constraints (5) maps into the the following constraint on the battery energy exchange  $-u_{d,\max} \leq u(k) \leq u_{c,\max}$ ,  $k = 0, \dots, M-1$ .

Finally, we can formulate the *energy management problem*  $\mathcal{P}_t$ , that has to be solved at each time step  $t$ ,  $t = 0, \dots, M-1$ , based on the latest estimate  $\hat{d}(k|t-1)$ ,  $k \in [t, M-1]$ , of the solar energy production in order to get the optimal management strategy for the storage  $u^*(k) = u_c^*(k) - u_d^*(k)$ ,  $k \in [t, M-1]$ :

$$\begin{aligned} & \min_{\{h(k), u_c(k), u_d(k)\}_{k=t, \dots, M-1}} \sum_{k=t}^{M-1} h(k) & (\mathcal{P}_t) \\ & \text{s.t: (2), (3), (4), (5), (6)} \\ & \max\{p_b(k)\hat{g}(k|t-1), p_s(k)\hat{g}(k|t-1)\} \leq h(k) & (7) \\ & k = t, \dots, M-1 \\ & U(M) \geq U_0 \end{aligned}$$

where  $p_b(k)$  and  $p_s(k)$  are, respectively, the price to buy and to sell at  $k$ ,  $U_0 \in [0.05, 0.95]\bar{U}$  is the stored energy at the beginning of the day and the last constraint is imposed to avoid the depletion of the storage at the end of the day. Since  $p_b(k) > p_s(k) > 0$ ,  $k = 0, \dots, M-1$ , (7) enforces the (positive) buy cost or the (negative) selling cost to be the lowest as possible, compatibly with the other constraints. The auxiliary variables  $h(k)$ ,  $k = t, \dots, M-1$ , are introduced to make the cost function linear. As for the constraints, they are all linear, except for (6) and (7). As for (6), it is automatically satisfied since choosing  $u(k) \neq 0$  with both  $u_c(k) \neq 0$  and  $u_d(k) \neq 0$  entails wasting some energy due to the fact that the round trip efficiency is smaller than 100% as modeled by  $\varepsilon_c < 1$  and  $\varepsilon_d > 1$  in (3). As for (7), it can be rephrased as two linear inequalities where the two arguments of the max operator are both upper bounded by  $h(k)$ .

Note that the solution to problem  $\mathcal{P}_t$  provides a control input sequence over the whole horizon  $[t, M-1]$ . However, according to the adopted predictive approach, only the control action  $u^*(t)$  is applied, and then, a new problem  $\mathcal{P}_{t+1}$  integrating the prediction  $\hat{d}(k|t)$ ,  $k \in [t+1, M-1]$ , updated based on the  $d(t)$  measurement is solved to determine the control action at time  $t+1$ , and so on. This is summarized in Algorithm 1 where  $E[d(k)]$  denotes the mean of the disturbance  $d(k)$ .

*Remark 1.* (uncertain load). If also the load is uncertain, a further disturbance contribution should be included in

---

### Algorithm 1 Energy management strategy

---

- 1: Set  $t = 0$  and  $\hat{d}(k|t-1) = E[d(k)]$ ,  $k = 0, \dots, M-1$
  - 2: **while**  $t \leq M-1$  **do**
  - 3:   Solve the optimization problem  $\mathcal{P}_t$  and calculate the control policy
 
$$u^*(k) = u_c^*(k) - u_d^*(k), \quad k = t, \dots, M-1$$
  - 4:   Apply  $u^*(t)$
  - 5:   Get the observation  $d(t)$
  - 6:   If  $t < M-1$ , then, update the prediction  $\hat{d}(k|t)$ ,  $k = t+1, \dots, M-1$ , of the future disturbance values over the residual time horizon  $[t+1, M-1]$
  - 7:    $t \leftarrow t+1$
  - 8: **end while**
- 

place of the deterministic signal  $\ell(k)$  and treated like the photovoltaic energy generation disturbance  $d(k)$ .  $\square$

We next describe the adopted time series predictor of the photovoltaic energy production.

### 3. PHOTOVOLTAIC ENERGY PREDICTION

Suppose that  $N$  daily profiles of photovoltaic energy production discretized into  $M$  time frames are available:

$$\{\mathbf{d}_n = [d_n(0), \dots, d_n(M-1)]^\top\}_{n=1}^N$$

We can then compute an estimate of the covariance matrix  $D$  of the stochastic variable  $\mathbf{d}$  as follows  $C = \frac{1}{N} \sum_{n=1}^N (\mathbf{d}_n - \bar{\mathbf{d}})(\mathbf{d}_n - \bar{\mathbf{d}})^\top$ , where  $\bar{\mathbf{d}}$  is the (estimated) mean  $\bar{\mathbf{d}} = \frac{1}{N} \sum_{n=1}^N \mathbf{d}_n$ . Since matrix  $C$  is real, symmetric, and positive definite, it can be factorized as follows  $C = V\Sigma V^\top$ , where  $\Sigma$  is diagonal and contains the  $M$  eigenvalues in decreasing order of magnitude:  $\Sigma_{ii} = \lambda_i$ ,  $\lambda_1 \geq \lambda_2 \geq \dots \geq \lambda_M$ . In turn,  $\Sigma$  can be factorized as  $\Sigma = \tilde{\Sigma}\tilde{\Sigma}^\top$ . Matrix  $C$  can thus be rewritten as  $C = (V\tilde{\Sigma})(V\tilde{\Sigma})^\top$ . The column of  $V$  are the eigenvectors of  $C$  and are called *Principal Components*. Each principal component is associated to an eigenvalue  $\lambda_i$ . The principal components associated with lower eigenvalues can be discarded with little loss of information. The dominant components of  $V$  can be selected by extracting the first  $H \leq M$  columns of  $V$  and defining matrix  $\Phi$ . One can select the dominant components by setting  $H$  as the minimum  $h$  such that  $\sum_{j=1}^h \lambda_j / \sum_{j=1}^M \lambda_j \geq \beta$ , where  $\beta \in (0, 1)$  is the amount of data variability that one wants to explain.

The stochastic variable  $\mathbf{d}$  can then be represented as

$$\mathbf{d} = \bar{\mathbf{d}} + \Phi\theta + e, \quad (8)$$

where  $\theta \in \mathfrak{R}^K$  are the (stochastic) *scores* of  $\mathbf{d}$  obtained via the orthogonal projection  $\theta = \Phi^\top(\mathbf{d} - \bar{\mathbf{d}})$  of  $\mathbf{d} - \bar{\mathbf{d}}$  onto the subspace  $\Phi$ , whereas  $e \in \mathfrak{R}^M$  is an additive noise that takes into account the approximation error due to both the estimation of the covariance matrix and the extraction of the principal components. The noise expression  $e = (I - \Phi\Phi^\top)(\mathbf{d}_n - \bar{\mathbf{d}})$  can be easily derived from (8), where  $I$  is the identity matrix of dimension  $M$ . Notice that  $e$  has zero expected value and variance

$$\Sigma_e = (I - \Phi\Phi^\top)V\Sigma V^\top(\Phi^\top\Phi - I). \quad (9)$$

The observation  $d(t)$  of the photovoltaic energy production in the time frame  $t$ ,  $t \in \{0, \dots, M-1\}$ , can be described

as the output of the following system with state given by the scores vector:

$$\begin{cases} \theta(t+1) = \theta(t) \\ d(t) = \Phi_t \theta(t) + \bar{d} + e(t) \end{cases} \quad (10)$$

where  $\Phi_t$  is the  $t$ -th row of  $\Phi$  and the scores vector are constant but not directly accessible. The idea is then to compute the conditional mean estimator  $\hat{\theta}(t|t)$  of the scores vector given the observations  $d(0), \dots, d(t)$ , which allows to build the desired predictor

$$\hat{d}(k|t) = \Phi_k \theta(t|t) + \bar{d}, \quad k = t+1, \dots, M-1.$$

In order to derive a filter for computing the conditional mean  $\theta(t|t)$ , we model the output error as an AutoRegressive (AR) process of order  $\eta$  (AR( $\eta$ )):

$$e(t+1) = \sum_{i=0}^{\eta-1} a_i e(t-i) + \epsilon(t), \quad \epsilon(t) \sim WN(0, \Gamma_{\epsilon t}). \quad (11)$$

The number and the values of parameters  $a_i$  in equation (11) can be chosen according to classical model identification theory criteria (i.e. looking at its autocorrelation and partial correlation functions). Notice that a time-varying variance for the process noise  $\epsilon(t)$  is assumed. The AR( $\eta$ ) process can be rewritten in state space form by defining the state vector  $\xi(t) = [e(t) \ \dots \ e(t-\eta+1)]^\top$ :

$$\xi(t+1) = \tilde{A}\xi(t) + \tilde{B}\epsilon(t), \quad (12)$$

where

$$\tilde{A} = \begin{bmatrix} a_1 & \dots & a_{\eta-1} & a_\eta \\ & I & & \mathbf{0} \end{bmatrix}, \quad \tilde{B} = [1 \ 0 \ \dots \ 0]^\top,$$

$I$  being the identity matrix of size  $\eta-1$  and  $\mathbf{0}$  a zeros matrix of appropriate dimensions (here a column vector of dimension  $\eta-1$ ). The generation mechanism (10) can then be extended to include (12), thus leading to

$$\begin{cases} \begin{bmatrix} \theta(t+1) \\ \xi(t+1) \end{bmatrix} = \begin{bmatrix} I & \mathbf{0} \\ \mathbf{0} & \tilde{A} \end{bmatrix} \begin{bmatrix} \theta(t) \\ \xi(t) \end{bmatrix} + \begin{bmatrix} \mathbf{0} \\ \tilde{B} \end{bmatrix} \epsilon(t) \\ d(t) = [\Phi_t \ \tilde{B}^\top] \begin{bmatrix} \theta(t) \\ \xi(t) \end{bmatrix}^\top + \bar{d} + \epsilon_2(t) \end{cases} \quad (13)$$

where  $\epsilon_2 \sim WN(0, \Sigma_{\epsilon_2})$  is a (small) measurements noise. We can rewrite model (13) using the compact notation

$$\begin{cases} x(t+1) = Ax(t) + B\epsilon(t) \\ d(t) = C_t x(t) + \bar{d} + \epsilon_2(t). \end{cases} \quad (14)$$

Unfortunately we cannot apply the Kalman filter to (14), since the distribution of the initial state  $x(0)$  is not Gaussian. We can model the non-Gaussian initial state  $x(0)$  by a Gaussian Mixture Model (GMM) with probability density function (pdf) given by  $f_{x(0)}(\cdot) = \sum_{j=1}^p \alpha_j \mathcal{G}(\cdot; \mu_j, \Gamma_j)$ , where  $\mathcal{G}(\cdot; \mu, \Gamma)$  denotes a multivariate Gaussian pdf over  $\mathbb{R}^{K+\eta}$  with mean  $\mu$  and covariance matrix  $\Gamma$ , whereas the  $\alpha_j$ 's coefficient belong to  $[0, 1]$  and sum up to 1.

The quantile-quantile (Q-Q) plots in Figure 2 refer to the first three components of the scores vector and are built based on the scores derived from empirical data and those extracted from the identified GMM with  $p=3$ . Since the plots describes a line with  $45^\circ$  slope, then, the GMM distribution correctly describes the scores of our dataset.

The a-posteriori GMM pdf of the state

$$f_{\hat{x}(t|t)}(\cdot) = \sum_{j=1}^p \alpha_j(t|t) \mathcal{G}(\cdot; \mu_j(t|t), \Gamma_j(t|t)) \quad (15)$$

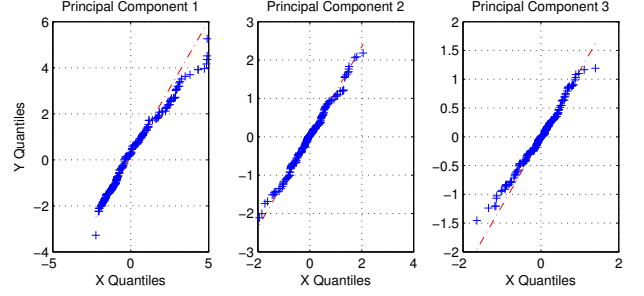


Fig. 2. Q-Q plots of the scores from a real data set and the scores from a data set extracted from a GMM.

can be determined recursively by the following Gaussian Mixture Kalman Filter (GMKF) (see Bilik and Tabrikian (2005) and Bilik and Tabrikian (2010)):

$$\mu_j(t|t) = \mu_j(t|t-1) + K_j(t)(d(t) - C_t \mu_j(t|t-1) - \bar{d})$$

$$\Gamma_j(t|t) = (I - K_j(t)C_t)\Gamma_j(t|t-1)$$

$$\alpha_j(t|t) = L_t^{-1} \alpha_j(t|t-1) \mathcal{G}(d(t); C_t \mu_j(t|t-1) + \bar{d},$$

$$C_t \Gamma_j(t|t-1) C_t^\top + \Gamma_{\epsilon_2})$$

$$\mu_j(t|t-1) = A \mu_j(t-1|t-1)$$

$$\Gamma_j(t|t-1) = A \Gamma_j(t-1|t-1) A^\top + \Gamma_\epsilon$$

$$\alpha_j(t|t-1) = \alpha_j(t-1|t-1),$$

where the Kalman gain and the likelihood  $L_t$  are given by

$$K_j(t) = \Gamma_j(t|t-1) C_t^\top (C_t \Gamma_j(t|t-1) C_t^\top + \Gamma_{\epsilon_2})^{-1}$$

$$L_t = \sum_{j=1}^p \alpha_j(t|t-1) \mathcal{G}(d(t); C_t \mu_j(t|t-1) + \bar{d},$$

$$C_t \Gamma_j(t|t-1) C_t^\top + \Gamma_{\epsilon_2}).$$

Based on the a-posteriori density (15), we can compute the conditional mean of  $x(k)$ ,  $k = t+1, \dots, M-1$ , as follows

$$\hat{x}(k|t) = A^{k-t} \hat{x}(t|t) = A^{k-t} \sum_{j=1}^p \alpha_j(t|t) \mu_j(t|t),$$

from which we finally get

$$\hat{d}(k|t) = C_k A^{k-t} \sum_{j=1}^p \alpha_j(t|t) \mu_j(t|t) + \bar{d}.$$

#### 4. VALIDATION OF THE PROPOSED STRATEGY

We consider the smart grid testbed in Figure 3 that was set up at GERC and consists of a photovoltaic panel installation with the associated inverter, a programmable load simulator, a battery storage unit with its inverter, and a grid interface. Four smart meters provide measures of the involved energy flows, with the meters of the photovoltaic installation and battery located downstream the corresponding inverters so as to include power conversion losses. A control interface is connected to the inverters via a serial RS485 interface for collecting monitoring data and also setting the energy exchange with the battery.

The load request along a one-day time horizon was set equal to the deterministic profile reported in Figure 4 (left plot), which was designed so as to resemble a typical residential load and rescaled in order to have a daily energy consumption equal to the average daily energy production from the considered photovoltaic panel installation.

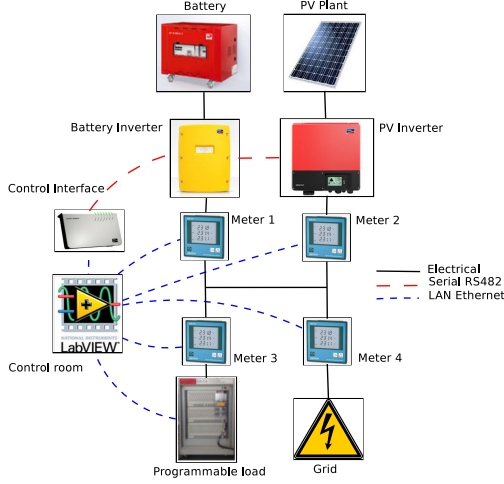


Fig. 3. Testbed layout.

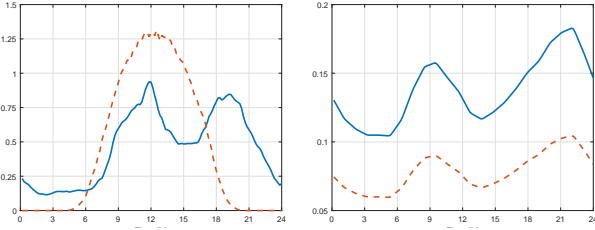


Fig. 4. Left: load (solid) and average photovoltaic (dashed) profiles [kW]. Right: buy (solid) and sell (dashed) electricity price [Euro/MJ]. Plots refer to a one-day time horizon.

To assess the performance of the proposed **optimal strategy**, we compared it against two alternative strategies:

**Heuristic strategy:** Battery is charged whenever it is not full and the produced energy exceeds the load request; battery feeds the load whenever it is not empty and the produced energy is lower than the load request. This policy is simple and is often implemented in commercial products;

**Best strategy:** Battery is optimally managed with the actual photovoltaic energy production profile in place of its prediction. This represents the best achievable performance for the battery management and can be computed via simulation a-posteriori.

The time slots duration was set equal to  $\Delta t = 10$  minutes, and, accordingly,  $M = 144$ . The price values in Figure 4 (right plot) are taken from the Italian daily national market electricity average profile with (to buy) and without (to sell) distribution costs and tax burdens. The highest selling price is lower than the lowest buying price, so that it is not economic to buy energy and sell it back later.

The storage capacity and the power charging/discharging rate are 6.8 kWh and 3.5 kW respectively, so that the storage can be charged at full power in about 2 hours (approximately 3.5 hours at rated photovoltaic power production) and can supply the load for about 8 hours. According to these specifications, we have the following parameters for  $\mathcal{P}_t$ ,  $\bar{U} = 24.48$  MJ, and  $u_{c,\max} = u_{d,\max} = 2.1$  MJ given the value for  $\Delta t$ . The energy exchanged with the storage affects its content according to model (3) whose parameters were identified through experiments. In

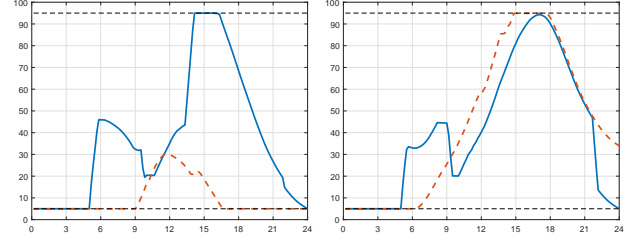


Fig. 5. Experiment 1: storage state of charge [in %] for the low photovoltaic energy production on August 11, 2016 (left) and the high photovoltaic energy production on August 16, 2016 (right), when applying the optimal (solid) and heuristic (dashed) strategies.

particular, we obtained  $\varepsilon_c = 1 - \varepsilon_u$  and  $\varepsilon_d = 1 + \varepsilon_u$  with  $\varepsilon_u = 0.02$ , and  $a = 0.999$ .

We validated our control strategy on the testbed, hardware in the loop, for the first 30 days of August 2016. The test was then repeated for the heuristic strategy, with the hardware in the loop, feeding the system with recorded photovoltaic signals instead of real measures. The best strategy was instead applied via simulation. We set the initial state of the storage as  $U(0) = 0.05\bar{U}$ , which is the optimal value for the periodic solution obtained for a deterministic set-up where the disturbance is equal to its mean profile. At the end of the day, both the Best and the Optimal strategies assign  $U(M) = U(0)$ . In order to make a fair comparison of the three approaches, in the case when the heuristic strategy at the end of the day has some energy stored in the battery ( $U(M) > U_{\min}$ ), this additional energy is converted into a (negative) contribution to the cost using the mean of the (selling) price.

Results are presented in the column Experiment 1 of Table 1. Electricity costs for the three different control strategies are presented for all 30 days, together with the total (*Tot.*), minimum (*Min.*), maximum (*Max.*) and average (*Avg.*) costs. Only a few times (e.g., days 28 and 30) the heuristic strategy outperforms the optimal strategy while the latter does better in most cases. In general, the optimal strategy gets a closer performance to the best performance than the heuristic strategy, and nearly a half of the achievable improvement. The optimal strategy allows a better usage of storage in days when the photovoltaic energy production is low (i.e. cloudy days) and the storage need to be charged using the grid to then feed the load when the electricity price is higher (Figure 5, left plot). On sunny days (Figure 5, right plot), the optimal strategy sells energy when the selling price is higher by anticipating the fact that the photovoltaic energy production is large and exceeds the load demand, while the heuristic strategy sells energy only when the battery is full, which does not necessarily happen in the most profitable time slots.

Evidently, at the start of the day observations are not informative regarding the possible high or low production and this motivates the unavoidable gap in performance between the optimal and the best strategy, where the profiles are perfectly known at the beginning of the day.

In Experiment 2, we investigated by simulation the performance of the strategies in the case of a smaller storage with capacity and power rate given by 3 kWh and 2 kW



Day	Experiment 1			Experiment 2		
	Best	Optimal	Heuristic	Best	Optimal	Heuristic
1	-0.74	-0.55	-0.49	-0.51	-0.43	-0.27
2	0.93	1.06	1.20	1.12	1.27	1.28
3	-1.20	-1.10	-0.85	-0.89	-0.88	-0.64
4	-0.94	-0.72	-0.64	-0.61	-0.58	-0.33
5	3.53	3.72	4.44	3.72	3.91	4.43
6	0.02	0.25	0.10	0.26	0.44	0.47
7	-1.19	-1.03	-0.84	-0.91	-0.86	-0.67
8	-1.33	-1.09	-0.95	-1.00	-0.99	-0.75
9	2.90	3.10	3.68	3.10	3.23	3.67
10	3.29	3.46	4.13	3.51	3.64	4.11
11	2.62	2.97	3.40	2.84	3.07	3.38
12	4.09	4.29	5.08	4.31	4.52	5.07
13	-1.15	-0.93	-0.81	-0.83	-0.81	-0.58
14	-0.85	-0.68	-0.57	-0.55	-0.53	-0.31
15	-0.62	-0.44	-0.40	-0.33	-0.29	-0.08
16	-0.62	-0.44	-0.40	-0.35	-0.29	-0.10
17	-0.84	-0.67	-0.57	-0.50	-0.46	-0.26
18	0.97	1.24	1.25	1.18	1.40	1.38
19	0.35	0.55	0.46	0.60	0.74	0.76
20	0.75	0.91	0.92	1.03	1.21	1.31
21	1.16	1.33	1.44	1.26	1.44	1.42
22	-0.61	-0.39	-0.40	-0.31	-0.25	-0.07
23	-0.87	-0.61	-0.59	-0.53	-0.47	-0.27
24	-0.99	-0.73	-0.68	-0.66	-0.59	-0.40
25	-0.93	-0.67	-0.64	-0.60	-0.54	-0.35
26	-0.69	-0.44	-0.45	-0.37	-0.30	-0.12
27	-0.62	-0.40	-0.39	-0.31	-0.24	-0.06
28	-0.03	0.28	0.07	0.23	0.38	0.45
29	2.75	3.02	3.53	2.93	3.04	3.52
30	0.36	0.60	0.37	0.60	0.71	0.70
Tot.	9.52	15.90	20.38	17.45	20.47	26.69
Min.	-1.33	-1.10	-0.95	-1.00	-0.99	-0.75
Max.	4.09	4.29	5.08	4.31	4.52	5.07
Avg.	0.32	0.53	0.68	0.58	0.68	0.89

Table 1. Results obtained on the testbed (columns ‘Optimal’ and ‘Heuristic’ of Experiment 1) and by simulation (column ‘Best’ of Experiment 1 and Experiment 2)

respectively, which can be charged at full power in approximately 1.5 hours (approximately 3 hours at rated solar power production) and can supply energy to the load for approximately 5 hours. Accordingly  $\bar{U} = 10.8$  MJ and  $u_{c,\max} = u_{d,\max} = 1.2$  MJ. Results are presented in the column ‘Experiment 2’ of Table 1. The optimal strategy achieves a performance that is closer to the best strategy limiting the degradation due to the reduced storage capacity, as shown in Figure 6 (right plot).

## 5. CONCLUSIONS AND OUTLOOK

In this paper a micro-grid energy management strategy is presented and its performance is validated on a lab testbed and via simulations. The proposed MPC-based strategy integrates a novel predictor of the uncertain photovoltaic energy production profile. Validation results show that the optimization of the energy management operations is particularly important in the case when the system has limited flexibility (storage with small capacity). They also point out the limits in the achievable performance posed by the inherent inaccuracy of a photovoltaic energy production predictor that relies only on measurement of the production profile, since at the beginning of the day

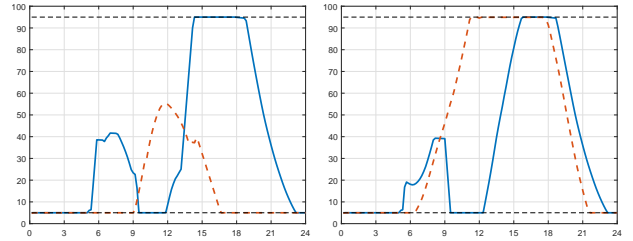


Fig. 6. Experiment 2: storage state of charge [in %] for the low photovoltaic energy production on August 11, 2016 (left) and the high photovoltaic energy production on August 16, 2016, when applying the optimal (solid) and heuristic (dashed) strategies.

they are not informative. Designing a predictor with better performance deserves further investigations.

## REFERENCES

- Bilik, I. and Tabrikian, J. (2005). Optimal recursive filtering using gaussian mixture model. In *IEEE/SP 13th Workshop on Statistical Signal Processing, 2005*, 399–404.
- Bilik, I. and Tabrikian, J. (2010). MMSE-based filtering in presence of non-Gaussian system and measurement noise. *IEEE Transactions on Aerospace and Electronic Systems*, 46(3), 1153–1170.
- Garcia, F. and Bordons, C. (2013). Optimal economic dispatch for renewable energy microgrids with hybrid storage using model predictive control. In *39<sup>th</sup> Conference of the IEEE Industrial Electronics Society*, 7932–7937.
- Ioli, D., Falsone, A., Hartung, M., Busboom, A., and Prandini, M. (2017). A smart grid energy management problem for data-driven design with probabilistic reachability guarantees. In G. Frehse and M. Althoff (eds.), *4th International Workshop on Applied Verification of Continuous and Hybrid Systems*, volume 48 of *EPiC Series in Computing*, 2–19.
- Manganini, G., Falsone, A., Siroky, J., and Prandini, M. (2017). A data-based approach to power capacity optimization. In *IEEE Conference on Decision and Control*, 1663–1668.
- Mesbah, A. (2016). Stochastic model predictive control: An overview and perspectives for future research. *IEEE Control Systems Magazine*, 36(6), 30–44.
- Olivares, D.E., Mehrizi-Sani, A., Etemadi, A.H., Caizares, C.A., Iravani, R., Kazerani, M., Hajimiragha, A.H., Gomis-Bellmunt, O., Saeedifard, M., Palma-Behnke, R., Jimnez-Estvez, G.A., and Hatziaargyriou, N.D. (2014). Trends in microgrid control. *IEEE Transactions on Smart Grid*, 5(4), 1905–1919.
- Pippia, T., Sijts, J., and De Schutter, B. (2018). A parametrized model predictive control approach for microgrids. In *IEEE Conference on Decision and Control*, 3171–3176.
- Ramsay, J.O. (2006). *Functional data analysis*. Wiley Online Library.
- Teleke, S., Baran, M.E., Huang, A.Q., and Bhattacharya, S. (2010). Optimal control of battery energy storage for wind farm dispatching. *IEEE Trans. on Energy Conversion*, 25(3), 787–794.
- Wan, C., Zhao, J., Song, Y., Xu, Z., Lin, J., and Hu, Z. (2015). Photovoltaic and solar power forecasting for smart grid energy management. *CSEE Journal of Power and Energy Systems*, 1(4), 38–46.
- Xie, L., Gu, Y., Eskandari, A., and Ehsani, M. (2012). Fast MPC-based coordination of wind power and battery energy storage systems. *J of Energy Engineering*, 138(2), 43–53.
- Zamora, R. and Srivastava, A.K. (2010). Controls for microgrids with storage: Review, challenges, and research needs. *Renewable and Sustainable Energy Reviews*, 14(7), 2009–2018.
- Zia, M.F., Elbouchikhi, E., and Benbouzid, M. (2018). Microgrids energy management systems: A critical review on methods, solutions, and prospects. *Applied Energy*, 222, 1033–1055.